by as much as ±0.02 e. The potential at the proton may be in error from this source by 0.1 to 0.2 eV and, since these appear to be random rather than systematic, the errors in the relative values of ΔV may be still larger. In spite of these difficulties, this analysis provides additional insight into the atomic contributions to the electrostatic potential shifts at the acidic proton.

First consider the total contributions of the monopole, dipole, and quadrupole moments to the electrostatic potentials at the acidic protons for formic and acetic acids. These numbers are given in the 6th and 13th rows of Table VII; the shifts, or differences, between these two sets of values are given in the 14th row (labeled ΔV). The monopole, or charge, contribution to ΔV is negative (−0.588 V) while the dipole and quadrupole contributions are both positive (+0.263 and +0.132, respectively). Therefore, it is the dominance of the charge contribution that produces the observed negative initial-state shift.

Second, consider the sum of each basin's monopole, dipole, and quadrupole contributions to the electrostatic potential at the acidic protons in formic and acetic acids. These values are given in the last column of Table VII. All carboxy group atoms contribute a negative shift to ΔV for acetic/formic acids [C1 (−0.295), O3 (−0.303), O4 (−0.062), H8-5 (−0.090)]; the substituent shift is positive (+0.557).

Now consider the individual monopole, dipole, and quadrupole contributions for each basin. Looking first at contributions from the basin quadrupole moments, we find that the only significant contribution from these to the potential at the hydrogen is from the hydroxy oxygen (O4). It is positive and becomes more so (+0.188 V) as the hydrogen is replaced with a methyl group. For the dipole moments, the hydroxy oxygen produces the only negative shift (−0.139). For the monopole, or charge contributions, all atoms contribute a negative shift except for the substituent. The charge on the methyl group in acetic acid is more positive than that on the substituent hydrogen in formic acid; the negative charge contributions arise from the electrons that have been transferred from the methyl group to the atoms of the carboxy group. The largest contributions arise from C1, the carboxy carbon, −0.45 V (because the charge there has become more negative by a relatively large amount, −0.07 e), and the carboxy oxygen, −0.32 V (because of its close proximity to the hydroxy oxygen). The charge and dipole contributions of the methyl group are positive; the quadrupole contribution is negligible. Thus, the methyl group makes its effect felt by contributing electrons to the polar carboxy group rather than through induction of a dipole moment (polarization) on the methyl group.

Conclusions

These experimental results show the influence of initial- and final-state effects on the relative gas-phase acidities of a series of carboxylic acids. The results for acetic, propionic, and butyric acids are as expected; the shift in final-state relaxation, relative to acetic acid, for these molecules is large and positive and the shift in initial-state is relatively small and negative. This is in keeping with the results of previous studies where molecules that differed primarily in polarizability were studied.

The anomalous gas-phase acidity of formic acid is attributed to a large, and dominating, initial-state potential shift. This is the reverse of what one might expect and the reverse of what is seen for other systems when hydrogen is replaced by a methyl group. Two factors contribute to this reversal. The effect of the methyl group on the initial-state potential is unusually large because the methyl group is attached to a very electronegative center—the carboxy carbon—and in the initial state, the methyl group is highly polarized and contributes electrons to the carboxy carbon. Relaxation effects are reduced from what is seen for other systems because the methyl group is relatively remote from the site where the positive charge is removed (from the hydroxy group).

The charge-distribution calculations show that the main effect of the alkyl substituent in the neutral acids is to reduce the high positive charge imposed on the carboxy carbon by the electronegative oxygen atoms through transfer of electrons to the carboxy group, and to accept electrons from the carboxy group during the relaxation to the final state.

Acknowledgment. We are pleased to acknowledge an interesting discussion with R. D. Topsom, which led to this work. We thank Andrew Streitwieser, Jr., for providing computer facilities. M.S. would like to thank David A. Shirley for support while this paper was being prepared. This work was supported in part by the National Science Foundation and the Department of Energy.

Registry No. Formic acid, 64-18-6; acetic acid, 64-19-7; propionic acid, 79-09-4; butyric acid, 107-92-6; methyl propionate, 554-12-1; methyl butyrate, 623-42-7; germane, 7782-65-2; formate anion, 71-47-6; acetate anion, 71-50-1; propionate anion, 72-03-7.

Supplementary Material Available: Listing of optimized geometries of formic acid, formate ion, acidic acid, acetate ion, and propionic acid together with the RHF-SCF energies (5 pages). Ordering information is given on any current masthead page.

An ab Initio Theoretical Reaction Path Study of the Cation Radical Diels–Alder Reaction

Nathan L. Bauld

Contribution from the Department of Chemistry, The University of Texas, Austin, Texas 78712.
Received March 8, 1991

Abstract: The theoretical reaction path for the Diels-Alder reaction of the *s-cis*-1,3-butadiene cation radical with ethene, yielding the cyclohexene cation radical, has been studied at the MP3/6-31G*//3-21G level. The results suggest a concerted, nonsynchronous, activationless cycloaddition in the gas phase.

The development of a diverse and synthetically useful body of cation radical chemistry has been the foremost priority of this research group for more than a decade.[1] The discovery of the aminium salt catalyzed Diels–Alder reaction, reinforced by the subsequent demonstration of the generality and synthetic utility of cation radical Diels–Alder reactions, asserted the relevance of cation radical pericyclic chemistry, and of the associated concept of hole catalysis, to organic synthesis.[2,3] Further implementation

(1) Bellville, D. J.; Wirth, D. D.; Bauld, N. L. *J. Am. Chem. Soc.* **1981**, *103*, 718–720.

(2) Bellville, D. J.; Bauld, N. L. *J. Am. Chem. Soc.* **1982**, *104*, 2665–2667. Since butadiene is more readily ionized than ethene, the [4+1] surface here is an excited state cation radical surface. To study a ground state [4+1] reaction, a dienophile more readily ionized than butadiene is required.

0002-7863/92/1514-5800$03.00/0

of this catalytic concept has permitted the development of a wide range of synthetically viable cation radical pericylic chemistry.[4,5] The mechanistic and theoretical aspects of these novel reactions are also of fundamental interest and have not been entirely neglected.[6,7] Mechanistically, a hole catalyst/initiator ($H^{\bullet+}$) removes an electron from a reactant molecule (R_1), generating a reactive cation radical ($R_1^{\bullet+}$). This latter species either rearranges intramolecularly or reacts with a second, neutral molecule (R_2) to give a product cation radical ($P^{\bullet+}$). The neutral product (P) is formed when $P^{\bullet+}$ removes an electron from either the neutral form (H) of the hole catalyst (the classic catalytic version of hole transfer catalysis) or from a neutral reactant molecule, R_1 (hole transfer chain catalysis). Theoretical interest has focused especially on (i) the basis for the overwhelming kinetic impetus of these reactions,[3,8] (ii) rationalization of their unique and highly developed selectivities,[2,9] and (iii) the question of concerted vs stepwise mechanisms.[2,8] Frontier orbital theory, orbital correlation diagrams, and semiempirical reaction path calculations have already provided useful insights into these and other questions. As early as 1980, a program was initiated in this laboratory to explore theoretical reaction paths of a variety of cation radical pericyclic chemistry on ab initio SCF MO and post SCF MO potential energy surfaces. The results of some of these investigations[3,8,10,11] as well as some from other laboratories have already been presented.[12] Final results for the cation radical Diels–Alder reaction, which involves the more formidable $C_6H_{10}^{\bullet+}$ surface, are now reported.

Results

Ab initio reaction paths of organic cation radicals having four or more carbon atoms were unknown at the start of this research. With the exception of preliminary accounts of the present work, calculations on cation radical systems having six or more carbon atoms still do not appear to have been reported. In our view, six carbon atoms represents the minimum number required to reflect even the most basic aspects of the efficient hole catalytic chemistry developed during the previous decade. In fact, six carbons do not permit convenient study of the *formally* symmetry allowed [4 + 1] Diels–Alder (neutral diene/dienophile cation radical), but the *formally* forbidden [3 + 2] Diels–Alder (diene cation radical/neutral dienophile) is readily amenable to study, and the results ultimately remove much of the motivation for pursuing the more demanding [4 + 1] path.[2] The computation of potential surfaces for cation radicals, and especially those of moderate size, is complicated by several factors. Obviously, spin doublets require the more time consuming UHF procedure. More critically, since activation barriers are typically so small in cation radical systems, these surfaces are highly compressed in the energy dimension, often by an order of magnitude or more, in comparison to corresponding neutral systems. Moreover, the barriers of real interest are now rarely very much larger than, and sometimes are even smaller than, the numerous torsional barriers. Though lacking in overall relief (energetically) cation radical surfaces seem to present an exceptional number of minute structural features (minima of ≤1 kcal/mol depth). Finally, a number of alternative reactions are also often accelerated on the compressed cation radical surface, making diversion to an undesired reaction path a likely possibility.

Chart I[a]

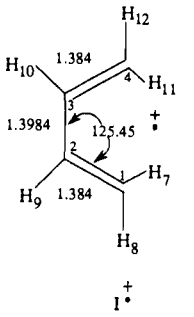

s-cis-1,3-Butadiene Cation Radical

[a] E(3-21G) = −153.7796 hartree, E(6-31G*) = −154.6477, E(MP2/6-31G*//3-21G) = −155.0984, E(MP3/6-31G*//3-21G) = −155.1372, E(PMP2) = −155.1072, $q_1 = q_4 = +0.36$; $q_2 = q_3 = +0.14$, $\rho_1 = \rho_4 = +0.11$; $\rho_2 = \rho_3 = -0.03$, $\phi(1,2,3,4) = 0.0047$ (~planar), q_i = net charge density on the ith carbon in the 3-21G basis set; hydrogen charges are added to those of the attached carbon, ρ_i = spin density on the ith carbon (au; 3-21G), ϕ = dihedral angle.

Chart II[a]

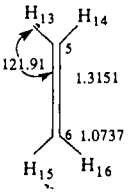

2

Ethene

[a] E(3-21G) = −77.6010, E(R) = −231.3805, E(6-31G*) = −78.0317, E(R) = −232.6794, E(MP2/6-31G*//3-21G) = −78.2841, E(R) = −233.3825, E(MP3/6-31G*//3-21G) = −78.3051, E(R) = −233.4423, E(R) = E(**1**$^{\bullet+}$) + E(**2**).

This may be especially problematic because the cation radical surface slopes predominantly downward from the reactants. As an example of the comparative difficulty of the present surface, it was observed quite early that the standard Berny method for geometry optimization could not successfully locate stationary points for many points on the $C_6H_{10}^{\bullet+}$ surface. In each case, however, the Murtaugh–Sargent algorithm, a slower and more reliable procedure, was found to optimize the points quite satisfactorily. For consistency, all points in this study were optimized using the latter method and then subjected to a final reoptimization using the more standard Berny algorithm. Further, the refinement of approximate transition states was virtually never possible without the calculation of analytic force constants at each stage of the optimization. Symmetry constraints were never employed, since it is well-known that cation radical reaction paths are highly unsymmetrical.[3,8] In view of all of these considerations, it was determined that optimization of the surface at a level higher than the 3-21G basis set would not be feasible. However, since correlation energy is known to be especially important in cation radical systems, all stationary points were recalculated at the MP2/6-31G*//3-21G level.[13] That correlation energy effects are well accounted for in the MP2 calculations was confirmed by comparison with MP3/6-31G*//3-21G calculations on the key stationary points. Finally, the effect of contaminating higher spin states on the stationary point energies was examined via the PMP2 spin projection method.

Some of the most essential calculated properties of the reactant system in the 3-21G basis set are illustrated in Charts I and II.

(3) Bauld, N. L.; Bellville, D. J.; Pabon, R. A.; Chelsky, R.; Green, G. *J. Am. Chem. Soc.* **1983**, *105*, 2378–2381.
(4) Bauld, N. L.; Bellville, D. J.; Harirchian, B.; Lorenz, K. T.; Pabon, R. A., Jr.; Reynolds, D. W.; Wirth, D. D.; Chiou, H. S.; Marsh, B. K. *Acc. Chem. Res.* **1987**, *20*, 371.
(5) Bauld, N. L. *Tetrahedron* **1989**, *45*, 5307–5363.
(6) Lorenz, K. T.; Bauld, N. L. *J. Am. Chem. Soc.* **1987**, *109*, 1157–1160.
(7) Reynolds, D. W.; Lorenz, K. T.; Chiou, H. S.; Bellville, D. J.; Pabon, R. A.; Bauld, N. L. *J. Am. Chem. Soc.* **1987**, *198*, 4960–4968.
(8) Bellville, D. J.; Bauld, N. L. *Tetrahedron* **1986**, *42*, 6167–6173.
(9) Bellville, D. J.; Bauld, N. L.; Pabon, R. A.; Gardner, S. A. *J. Am. Chem. Soc.* **1983**, *105*, 3584–3588.
(10) Bauld, N. L.; Pabon, R. A. *J. Am. Chem. Soc.* **1984**, *106*, 1145–1146.
(11) Bellville, D. J.; Chelsky, R.; Bauld, N. L. *J. Am. Chem. Soc.* **1982**, *3*, 548–551.
(12) Heinrich, N.; Koch, W.; Morrow, J. C.; Schwarz, H. *J. Am. Chem. Soc.* **1988**, *110*, 6332.
(13) Bouma, W. J.; Poppinger, D.; Radom, L. *J. Mol. Struct.* **1982**, *12*, 209.

Chart III[a]

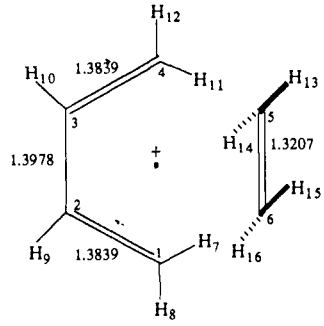

$3^{+\bullet}$

Sigma Ion Dipole Complex

[a] E(3-21G) = −231.3897, E(6-31G*) = −232.6870, E(MP2) = −233.3934, E(MP3) = −233.4528, E(PMP2) = −233.4021, $R_{4,5}$ = 3.8146, $R_{1,6}$ = 3.8624, $R_{5,11}$ = 2.7570, $R_{6,7}$ = 2.8117, Δy_5 = +0.66 (down), Δy_6 = −0.66 (up), q_1 = 0.35, q_4 = 0.35, q_2 = 0.13, q_3 = 0.13, q_5 = q_6 = 0.019, ρ_1 = 0.11, ρ_4 = 0.11, ρ_2 = −0.028, ρ_3 = −0.028; ρ_5, ρ_6 = 0.00, Δy_i = displacement above (+) or below (−) the C_1–C_2–C_3 plane for the ith atom.

Chart IV[a]

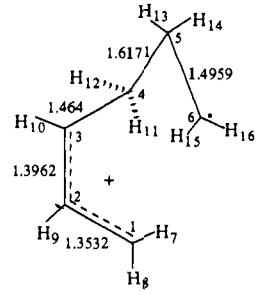

$4^{+\bullet}$

3-21G/ DIELS-ALDER INTERMEDIATE

[a] E(3-21G) = −231.3955, E(6-31G*) = −232.6877, E(MP2) = −233.4069, E(MP3) = −233.4617, E(PMP2) = −233.4119, $R_{1,6}$ = 3.1752, $R_{3,6}$ = 3.0511, ϕ(1,2,3,4) = −4.5861, ϕ(2,3,4,5) = −91.0405, ϕ(3,4,5,6) = 74.6138, q_1 = +0.4188, q_2 = −0.0275, q_3 = +0.3773, q_4 = +0.0352, q_5 = +0.0825, q_6 = +0.1135, ρ_1 = −0.0074, ρ_2 = 0.0007, ρ_3 = 0.0144, ρ_4 = 0.0533, ρ_5 = −0.0537, ρ_6 = 0.2172.

The *s-cis*-1,3-butadiene cation radical ($\mathbf{1}^{+\bullet}$) is of course planar (the dihedral angle $\phi_{1,2,3,4} \approx 0$) as expected for maximum delocalization of the singly occupied MO or SOMO (i.e., of the hole). The net positive charge density (q_i) is concentrated predominantly at the terminal carbons (see q_1, q_4) as compared to the internal carbons (see q_2, q_3), also as expected from the SOMO distribution, which is qualitatively that of the well-known neutral diene HOMO. The ratio q_1/q_2 = 2.56. Interestingly, the spin density, which *in the SOMO* is fully coupled to the charge density, is not similarly shared by the two sets of carbon atoms. The positive spin exists, so far as the carbon framework is concerned, only on the terminal carbons. The internal carbons actually have a small net *negative* spin density. Although such negative spin densities at carbon in doublet species are not at all unusual, it is more commonly the case that such atoms occupy nodal positions in the SOMO. It appears surprising that non-nodal atoms with a very substantial *positive* spin density contribution from the SOMO would have a net negative spin density. In any case it is interesting that spin and charge densities appear, at this level as well as at the MP3 level, to be significantly uncoupled even in this simple hydrocarbon cation radical. Although both effects should strongly favor reaction at a terminal carbon, spin effects would appear to do so even more decisively than charge effects. Finally, the C_1–C_2 and C_3–C_4 carbon–carbon bond lengths indicate modest weakening with respect to that of ethene (**2**), but the C_2–C_3 bond length is much strengthened relative to neutral 1,3-butadiene and only a little weaker than the C_1–C_2 bond, as expected for hole formation in a diene HOMO. Consequently, it is clear that rotation around any of these bonds, and most notably the C_2–C_3 bond, which interconverts **1** into its corresponding s-trans isomer, will be very difficult, especially in view of the generally low activation barriers for competing cation radical reactions.

In the earliest phase of this project, calculations were carried out using GAUSSIAN 76, a very early version in the GAUSSIAN series, on the University of Texas Dual Cyber 170/150 System.[14] The 3-21G basis set was also quite new and was necessarily input as an external basis set.[15] Worst of all, the geometry optimizations required repetitive cycles of one at a time variable optimization. The continuation of these studies has subsequently used virtually every new GAUSSIAN version up to and including GAUSSIAN 90. Considering the complexity of the $C_6H_{10}^{+\bullet}$ surface, it now seems almost astounding that the early results, reported in a preliminary way elsewhere, had any validity at all.[8] Nevertheless the key stationary points on the Diels–Alder surface not only remained in place but seem to have been affected relatively little. A minor exception is the π complex ($R_{4,5}$ = 3.35, $R_{1,6}$ = 3.99) from which the reaction path was staged. Using the analytical gradient methods available in later GAUSSIAN versions, this π complex could not be confirmed as an energy minimum. Instead, the geometry optimized all the way to a σ ion–dipole complex ($\mathbf{3}^{+\bullet}$; Chart III). The nearest carbon–carbon and carbon–hydrogen approaches between the two moieties of $\mathbf{3}^{+\bullet}$ are all approximately 2.5 times the normal bond length of the appropriate C–C or C–H bond type. Consequently, significant covalent interactions between the moieties is rendered unlikely. This conclusion is decisively confirmed by the charge and spin distributions in $\mathbf{3}^{+\bullet}$, which are essentially unperturbed from those in $\mathbf{1}^{+\bullet}$. In the preferred approach, the trigonal planes of $\mathbf{1}^{+\bullet}$ and **2** are approximately perpendicular, with H_7 and H_{11} projecting toward the π bond of **2**. The carbon atoms of **2** lie approximately in the trigonal plane of $\mathbf{1}^{+\bullet}$, but one carbon projects slightly above and one slightly below that plane. It is important to recall, however, that the energies of ion–dipole complexes are typically not highly geometry dependent, and the existence of other relative minima of this type is not considered unlikely.[12] Perhaps the most interesting aspect of the calculations on $\mathbf{3}^{+\bullet}$ is its binding energy, which is 6.6 kcal/mol at the MP3 level. The typical translational entropy change for the formation of a bimolecular encounter complex in solution is ca. −18 eu, the equivalent of a +5.4 kcal/mol contribution to the free energy.[16] The ion–dipole complex would thus appear to be slightly bound on a free energy surface which neglects solvation energies.

Beginning with $\mathbf{3}^{+\bullet}$ and adopting the $R_{4,5}$ coordinate as the reaction coordinate, the minimum energy reaction path (MERP) is noteworthy mainly for its flatness. As the distance is decreased from the value in $\mathbf{3}^{+\bullet}$ (3.8146) to 3.20 Å, the energy increases by only ca. 2 kcal/mol and then begins to decrease again. The energy maximum at 3.20 Å was rather carefully defined but despite extensive efforts could not verified as a saddle point. In this case, it appears that the difficulty may arise from the extremely rapid change in geometry with small changes in $R_{4,5}$ as the structure moves from a σ to a π complex. Nevertheless, the barrier is quite small, well below the initial reaction state energy, and eventually does not lead to a DA reaction path. Consequently the strategy originally used to pursue the Diels–Alder path turns

(14) Binkley, J. S.; Frisch, M. J.; DeFrees, D. J.; Rahgavachari. K.; Whiteside, R. A.: Schlegel, H. B.; Fluder, E. M.; Pople, J. A. Department of Chemistry, Carnegie-Mellon University, Pittsburgh, PA.

(15) Binkley, J. S.; Pople, J. A.; Hehre, W. J. *J. Am. Chem. Soc.* **1980**, *102*, 939.

(16) Ritchie, C. D. *Physical Organic Chemistry*, 2nd ed.; Marcel Dekker, Inc.: New York, 1990; p 132.

Chart V[a]

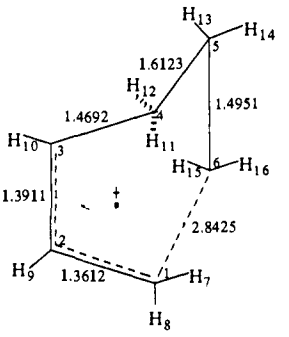

$5^{\ddagger}$

3-21G DIELS-ALDER TRANSITION STATE

[a] E(3-21G) = −231.3949, E(6-31G*) = −232.6871, E(MP2) = −233.4081, E(MP3) = −233.4631, E(PMP2) = −233.4155, q_1 = +0.40, q_2 = 0.00, q_3 = +0.34, q_4 = +0.04, q_5 = +0.09, q_6 = +0.13, ρ_1 = −0.03, ρ_2 = 0.00, ρ_3 = +0.05, ρ_4 = +0.03, ρ_5 = +0.04, ρ_6 = +0.20.

Table I. Relative Energies of Stationary Points on the Diels–Alder Path

	relative energy (kcal/mol)				
structure	3-21G	6-31G*	MP2	MP3	PMP2
1$^{\bullet+}$ + **2**	0.0	0.0	0.0	0.0	0.0
3$^{\bullet+}$	−5.7	−4.8	−6.6	−6.6	−6.7
4$^{\bullet+}$	−9.4	−5.9	−15.3	−12.2	−12.9
5$^{\bullet+}$	−9.0	−4.8	−16.1	−13.1	−15.2
6$^{\bullet+}$	−38.0[a]				

[a] Not fully optimized.

out to be the most effective one. The π complex type structure, though not an energy minimum, is important for staging the DA reaction path. Beginning with the π complex structure in which the ethene moiety is at least properly oriented for a possible Diels–Alder reaction and again choosing $R_{4,5}$ as the reaction coordinate, the Diels–Alder MERP is indeed tracked. Without encountering further energy minima the path descends directly to an intermediate (**4**$^{\bullet+}$) of the type which has been termed singly linked by Roth, i.e., the C_4–C_5 bond is essentially fully made, while the C_1–C_6 bond has essentially not yet begun to form (Chart IV). In the operative 3-21G basis set, a significant C_1–C_6 interaction is not indicated by either the C_5–C_6 torsional barrier or the existence of a structural minimum. The conclusion of the DA path requires conversion to an $R_{1,6}$ reaction coordinate. Closure of the C_1–C_6 bond passes through a saddle point (**5**$^{\bullet+}$; Chart V) at only 0.4 kcal/mol above **4**$^{\bullet+}$ and passes on to the cyclohexene cation radical. The transition state was verified not only via force constants but by optimization of a point just beyond the TS all the way to the DA adduct. An activation barrier of 1.1 kcal/mol is retained in point calculations for **4**$^{\bullet+}$ and **5**$^{\bullet+}$ at the 6-31G* level, but at the MP2/6-31G*//3-21G level **5**$^{\bullet+}$ is 0.8 kcal/mol more stable than **4**$^{\bullet+}$ (Table I). The MP3/6-31G*//3-21G calculation gives virtually the same energy difference (0.9 kcal/mol) as the MP2 calculations. With spin projection (PMP2), **5**$^{\bullet+}$ is 2.3 kcal/mol more stable than **4**$^{\bullet+}$. Finally, even if the π approach with a gauche conformation around the C_4–C_5 bond does favor a concerted reaction, it is of substantial interest to learn just how favored this gauche approach might be relative to others, particularly with an anti conformation about C_4–C_5. To explore this question, the torsional surface about the C_4–C_5 bond was explored at the 3-21G level and point calculations performed at the MP3/6-31G*//3-21G level (Table II). The torsional barrier (3.2 kcal/mol) emerges at quite normal for an sp^3–sp^3 carbon–carbon bond, but the gauche conformation (**4**$^{\bullet+}$) replaces the typical anti conformation as the global minimum. The energy difference is not very large (0.7 kcal/mol) in the 3-21G basis set but is more substantial at the higher levels of calculation (MP2, 2.0; MP3, 1.8; PMP2, 1.6).

Table II. Conformational Analysis of **4**$^{\bullet+}$: Possible Stepwise Reaction Paths

dihedral angle	ϕ (deg)	E(3-21G)	E(MP2)	E(MP3)	E(PMP2)
H_{15}–C_6–C_5–H_{13}	15 (“**4**$^{\bullet+}$”)	0.0	0.0	0.0	0.0
	45	0.45			
	75	1.2			
	120	1.8	2.1		
C_6–C_5–C_4–C_3	74 (“**4**$^{\bullet+}$”)	0.0	0.0		
	90	0.6			
	110	2.4			
	130	3.2			
	150	2.3	2.5		
	180	0.7	2.0	1.8	1.6

Chart VI. The 3-21G Cation Radical Diels–Alder Reaction Path

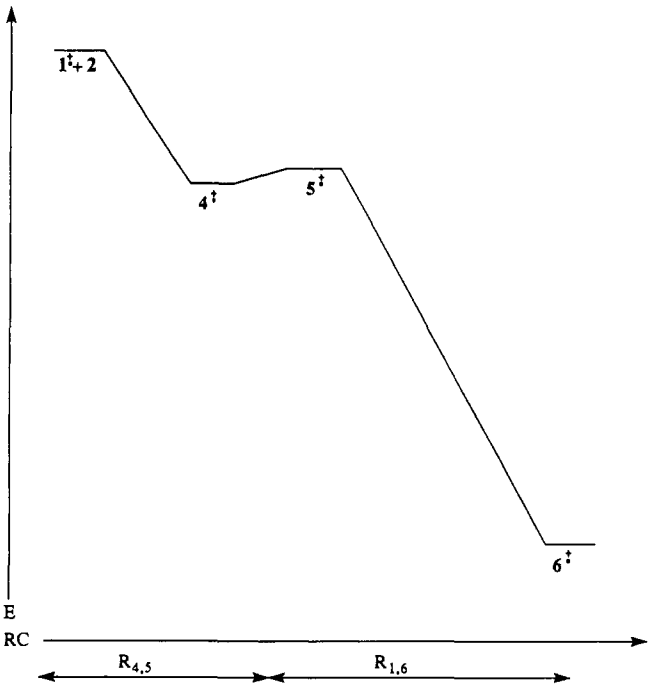

Discussion

The minimum energy reaction path (MERP) for the Diels–Alder cycloaddition of the *s-cis*-1,3-butadiene cation radical (**1**$^{\bullet+}$) to ethene (**2**) has been defined using the 3-21G basis set (Chart VI and Table I). This path is formally stepwise, proceeding through an intermediate (**4**$^{\bullet+}$) which has the character of an allylic carbocation moiety hyperconjugatively coupled via the newly formed C_4–C_5 bond to a primary radical moiety (Chart IV). The reaction which produces **4**$^{\bullet+}$ occurs without activation and also without the intervention of other intermediates, such as a π complex. The hyperconjugative coupling of the two moieties in **4**$^{\bullet+}$ has significant structural consequences. The C_4–C_5 bond is, of course, elongated to 1.62 Å. Perhaps more significantly, the enhanced π character of the C_5–C_6 bond substantially increases the torsional barrier for this bond and even qualitatively changes the conformational preference. By way of comparison, the torsional barriers for the sp^2–sp^3 carbon–carbon bond of primary radicals are extremely small (0.42 kcal/mol, e.g., for the propyl radical) and favor the positioning of the γ alkyl group in the trigonal plane of the radical center.[18] The primary radical site in **4**$^{\bullet+}$, in contrast, gives rise to a substantially larger torsional barrier with respect to the C_5–C_6 bond (1.8 kcal/mol) and prefers the conformation in which the bond to the γ alkyl group (the C_4–C_5 bond) is elipsed with the p orbital at the radical site (Table II). The latter conformation, of course, maximizes the proposed hyperconjugative interaction. The closure of **4**$^{\bullet+}$ to the cyclohexene cation radical (**6**$^{\bullet+}$) occurs with a miniscule barrier of 0.4 kcal/mol. Since the C_5–C_6 torsional barrier is significantly larger than this,

the cycloaddition should be stereospecific even on the formally stepwise 3-21G path. Although calculation of the energies of the stationary points on this MERP at the 6-31G*//3-21G level reveals no important changes, the MP2/6-31G*//3-21G energies now place the 3-21G transition state ($5^{\bullet+}$) at 0.8 kcal/mol below the intermediate ($4^{\bullet+}$). The same ordering and virtually the same energy difference are confirmed at the MP3/6-31G*//3-21G level (0.9 kcal/mol).

The path studied here represents a gauche approach of **2** to $1^{\bullet+}$ with reference to the C_4–C_5 bond. This approach, appropriately, permits but does not enforce simultaneous formation of both new carbon–carbon bonds. An intermediate ($4^{\bullet+}$) is located on the 3-21G reaction path, but the existence of a barrier to the cyclization of $4^{\bullet+}$ is not supported by the MP2 and MP3/6-31G*//3-21G stationary point calculations. A concerted reaction path is therefore suggested, but because the path is not fully optimized at the MP2 or MP3 level this conclusion must be considered tentative. If a concerted path is indeed favored, the gauche approach of **2** to $1^{\bullet+}$, which is implicit in the concerted Diels–Alder path, would be expected to be favored over approaches (especially, anti) which do not permit concert. A study of the torsional potential of the C_4–C_5 bond in $4^{\bullet+}$ confirms this prediction and further supports the proposed concerted mechanism (Table II). As expected for an sp^3–sp^3 carbon–carbon bond involving primary carbons, both gauche and anti minima are found. In sharp contrast to standard conformational preferences, however, the gauche conformer ($4^{\bullet+}$) is actually preferred over the corresponding anti conformation by ca. 2 kcal at the highest levels of theory applied.[18]

The present study finds no ion–dipole or π complex intermediates on the Diels–Alder cycloaddition path. Although a σ ion–dipole complex ($3^{\bullet+}$) lying in a very shallow minimum was located, no direct route to Diels–Alder addition from this intermediate could be found. The energetics of the formation of $3^{\bullet+}$ are nevertheless of interest in connection with the magnitudes of ion–dipole stabilization effects in cation radical-neutral reactions. Complex $3^{\bullet+}$ lies 6–7 kcal/mol below the reactants in the gas phase. Since the loss of translational entropy in an encounter complex is equivalent to an entropic destabilization of ca. 5 kcal/mol, the formation of $3^{\bullet+}$ is exergonic by just 1–2 kcal/mol.[16] In solution, particularly in polar solvents, the stabilization is undoubtedly further diminished.

The present study envisions a concerted, nonsynchronous, activationless Diels–Alder cycloaddition in the gas phase. In solution, DA cycloaddition rates within a factor of 60 of the diffusion controlled rate have been observed, indicating an activation energy of ca. 1–2 kcal/mol.[19] Since the corresponding neutral Diels–Alder reaction has an activation energy of >30 kcal/mol, it is evident that hole formation in **1** has essentially completely expunged a rather formidable barrier. An effect of this magnitude is clearly of theoretical interest. It is evident from the calculations that ion–dipole stabilization plays a major role in facilitating the cation radical/neutral reaction. The ion–dipole stabilization of 6–7 kcal/mol at a distance of 4.0 Å will be very substantially increased as the distance is closed. The resulting large ion–dipole attraction is more than adequate to dominate the usual nonbonded repulsions in the early stages of the reaction. Additional effects have previously been proposed to provide stabilization further along the reaction path but are not as readily assessed quantitatively from these calculations. It is worthwhile to stress that the kinetic impetus of the cation radical Diels–Alder relative to the corresponding neutral reaction is not derived from thermodynamic driving force, expressed as product character development in the transition state. On the contrary, the neutral reaction actually has the more favorable thermodynamics. On the other hand, product development factors may well favor the cation radical Diels–Alder reaction over the corresponding cation radical cyclobutanation.

Acknowledgment. The author thanks the University of Texas Center for High Performance Computation for generous allotments of computer time. The research was supported by the NSF (CHE-8822051) and the Robert A. Welch Foundation (F-149).

Registry No. $1^{\bullet+}$, 34488-62-5; **2**, 74-85-1; $4^{\bullet+}$, 141583-46-2; $6^{\bullet+}$, 34469-90-4.

Supplementary Material Available: Tables of optimized parameters and frequencies (46 pages). Ordering information is given on any current masthead page.

(17) Roth, H. D.; Schilling, M. L. *J. Am. Chem. Soc.* **1985**, *107*, 716.
(18) Edge, D. J.; Kochi, J. K. *J. Am. Chem. Soc.* **1972**, *94*, 6485–6495.
(19) Calhoun, G. C.; Schuster, G. B. *J. Am. Chem. Soc.* **1984**, *106*, 6870.